Marcel Junige, Tim Oddoy, Rositsa Yakimova, Vanya Darakchieva, Christian Wenger, Grzegorz Lupina, Julia Kitzmann, Matthias Albert, Johann W. Bartha

Atomic layer deposition of Al2O3 on NF3-pre-treated graphene

Erstveröffentlichung in / First published in:

SPIE Microtechnologies. Barcelona, 2015. Bellingham: SPIE, Vol. 9519 *[Zugriff am: 22.05.2019]*.

DOI: https://doi.org/10.1117/12.2181242

Atomic layer deposition of Al2O3 on NF3-pre-treated graphene

Marcel Junige, Tim Oddoy, Rositsa Yakimova, Vanya Darakchieva, Christian Wenger, et al.

Marcel Junige, Tim Oddoy, Rositsa Yakimova, Vanya Darakchieva, Christian Wenger, Grzegorz Lupina, Julia Kitzmann, Matthias Albert, Johann W. Bartha, "Atomic layer deposition of Al2O3 on NF3-pre-treated graphene," Proc. SPIE 9519, Nanotechnology VII, 951915 (1 June 2015); doi: 10.1117/12.2181242

SPIE.

Event: SPIE Microtechnologies, 2015, Barcelona, Spain

Atomic Layer Deposition of Al_2O_3 on NF_3-pre-treated graphene

Marcel Junige[a], Tim Oddoy[a], Rositsa Yakimova[b], Vanya Darakchieva[b], Christian Wenger[c], Grzegorz Lupina[c], Julia Kitzmann[c], Matthias Albert[a], and Johann W. Bartha[a]

[a] Technische Universität Dresden, Institute of Semiconductors and Microsystems (IHM), 01062 Dresden, Germany;
[b] Linköping University, Department of Physics, Chemistry and Biology (IFM), Semiconductor Materials, Linköping University, SE-58183, Linköping, Sweden;
[c] IHP GmbH – Leibniz institute for innovative microelectronics, Im Technologiepark 25, 15236 Frankfurt (Oder), Germany

ABSTRACT

Graphene has been considered for a variety of applications including novel nanoelectronic device concepts. However, the deposition of ultra-thin high-k dielectrics on top of graphene has still been challenging due to graphene's lack of dangling bonds. The formation of large islands and leaky films has been observed resulting from a much delayed growth initiation. In order to address this issue, we tested a pre-treatment with NF_3 instead of XeF_2 on CVD graphene as well as epitaxial graphene monolayers prior to the Atomic Layer Deposition (ALD) of Al_2O_3. All experiments were conducted in vacuo; i. e. the pristine graphene samples were exposed to NF_3 in the same reactor immediately before applying 30 (TMA$-H_2O$) ALD cycles and the samples were transferred between the ALD reactor and a surface analysis unit under high vacuum conditions. The ALD growth initiation was observed by in-situ real-time Spectroscopic Ellipsometry (irtSE) with a sampling rate above 1 Hz. The total amount of Al_2O_3 material deposited by the applied 30 ALD cycles was cross-checked by in-vacuo X-ray Photoelectron Spectroscopy (XPS). The Al_2O_3 morphology was determined by Atomic Force Microscopy (AFM). The presence of graphene and its defect status was examined by in-vacuo XPS and Raman Spectroscopy before and after the coating procedure, respectively.

Keywords: Atomic Layer Deposition (ALD), Aluminium(III) oxide (Al_2O_3), graphene, in-vacuo pre-treatment, Nitrogen trifluoride (NF_3), in-situ real-time Spectroscopic Ellipsometry (irtSE), in-vacuo X-ray Photoelectron Spectroscopy (XPS), Atomic Force Microscopy (AFM)

1. INTRODUCTION

Graphene is a two-dimensional Carbon monolayer with expected unique properties. Consequently, novel nanoelectronic device concepts have been reported such as the Graphene Base Transistor (GBT).[1] However, the deposition of ultra-thin films on top of graphene has still been challenging: On the one hand, the deposition process must not damage or alter the pristine graphene monolayer; on the other hand, the finally deposited films have to provide appropriate functional properties regarding a specific application. In case of the GBT, a dielectric coating has been desired which is both pinhole free to prevent any short circuits and still thin enough (around 3-5 nm) to enable hot electron tunneling. Hence, the dielectric film closure on graphene needs to occur at an early stage of the deposition process.

Atomic Layer Deposition (ALD) has been established for the last decade as a physicochemical coating technique with an excellent thickness control, unique conformality over complex three-dimensional-shaped substrates, as well as superior film quality at comparably lower deposition temperatures.[2–4] Especially the ALD of oxides has been extensively researched. Accordingly, an ALD process for Al_2O_3 has yet existed.[5]

Further author information: (Send correspondence to Marcel Junige)
Marcel Junige: E-mail: marcel.junige@tu-dresden.de, Telephone: +49 163 5809233

Nanotechnology VII, edited by Ion M. Tiginyanu, Proc. of SPIE Vol. 9519, 951915
 · doi: 10.1117/12.2181242

However, the ALD of Al_2O_3 has been reported to barely initiate on pristine graphene due to graphene's lack of dangling bonds. A functionalization using Xenon difluoride (XeF_2) has been found to provide additional nucleation sites resulting in conformal films without pinholes.[6] Per contra, XeF_2 (a solid at room temperature) is a very toxic and strong oxidizing agent, which may ignite or explode on contact with combustible materials.[7] Hence, the scope of our study was to test an alternative fluorinating agent, such as the comparably milder Nitrogen trifluoride (NF_3), which is a gas at room temperature and has been widely established in the microelectronics industry.

2. EXPERIMENTAL SETUP AND METHODOLOGIES

At IHP GmbH (Frankfurt (Oder), Germany), a commercially available Chemical Vapor Deposition graphene (CVD-G) monolayer (1 cm × 1 cm) was transferred from Copper onto a Silicon wafer coupon with 100 nm SiO_2 using a poly(methylmethacrylate) (PMMA)-assisted method as described in Ref. 8. At the Linköping University (Linköping, Sweden), an epitaxial graphene (EG) monolayer (0.7 cm × 1 cm) was prepared by sublimation of Silicon Carbide (SiC) and subsequent graphene formation on Si-face n-type 4H-SiC as published in Ref. 9, 10.

The Al_2O_3 ALD used the organometallic precursor trimethylaluminum (TMA) and the co-reactant water (H_2O) at a substrate set-point temperature of 400 ℃ and a total process pressure of 200 Pa. Each of the 30 consecutively applied ALD cycles repeated a sequence alternating 5 s TMA exposure, 30 s Ar purge, 5 s H_2O exposure, and 30 s Ar purge. In order to gain a high NF_3 reactivity, CVD-G was consecutively exposed to NF_3 for 180 s at stepwise elevated substrate temperatures. The Fluorine content was determined by in-vacuo XPS after each NF_3 exposure step. This revealed an optimum temperature for the NF_3-pre-treatment around 400 ℃, where most Fluorine was attached but the CVD-G remained intact.[11]

The utilized FHR-ALD-300 reactor (by FHR Anlagenbau GmbH, Ottendorf-Okrilla, Germany) was equipped with a M 2000® FI Rotating Compensator Ellipsometer (by J. A. Woollam. Co., Lincoln, Nebraska, USA). The ellipsometer windows were protected against the reactor's gas phase by purging the tubular view ports with a laminar Ar gas flow (no shutters were implemented). We have recently developed an in-situ real-time Spectroscopic Ellipsometry (irtSE) algorithm that enabled the acquisition of entire ellipsometric (Ψ, Δ) spectra (250-1700 nm) with a sampling rate above 1 Hz.[12–14] This allowed the in-situ real-time monitoring and control of kinetic processes (like precursor adsorption, ligand removal, and purging behavior) in ALD.[15] The ALD reactor chamber was also clustered to a Multiprobe® Ultra High Vacuum (UHV) system (by Omicron Nanotechnology GmbH, Taunusstein, Germany) for direct surface analysis like X-ray Photoelectron Spectroscopy (XPS) or Atomic Force Microscopy (AFM) at the same sample surface without breaking a high vacuum around 10^{-5} Pa during in-vacuo sample transfer. This entire experimental setup has particularly been described in Ref. 16, 17.

3. RESULTS

3.1 In-situ real-time Spectroscopic Ellipsometry (irtSE)

The Figures 1-3 show the optical Al_2O_3 layer thickness as determined by irtSE in progression over the ALD process time.

In Fig. 1, the ALD started on a 100 nm SiO_2 reference substrate. When the initial SiO_2 surface was pre-cleaned in O_3 for 180 s at 400 ℃, a nearly congruent optical thickness increment per cycle (commonly referred to as growth per cycle, GPC) was observed already starting from the very first ALD cycle. When the initial SiO_2 surface was pristine or pre-treated in NF_3 for 180 s at 400 ℃, the GPC as well as the optical thickness increment per TMA exposure was reduced for the very first 5 ALD cycles compared to the following homogeneous linear growth regime.

In Fig. 2, the ALD started on a 100 nm SiO_2 substrate supporting a CVD-G monolayer. The GPC on CVD-G was distinctly lower over the entire course of all 30 applied ALD cycles compared to the O_3-pre-cleaned (bare) SiO_2 reference. The optical thickness increment during the very first TMA exposure was especially reduced. No significant difference was observable by irtSE when the initial CVD-G was pristine or pre-treated in NF_3 for 180 s at 400 ℃.

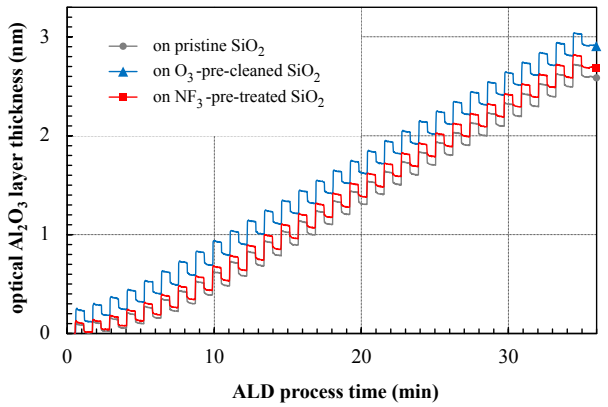

Figure 1. (color online) Optical Al_2O_3 layer thickness as determined by in-situ real-time Spectroscopic Ellipsometry (irtSE) in progression over the (TMA−H_2O, 400 ℃) ALD process time starting on a 100 nm SiO_2 reference substrate that was initially pristine (•), initially pre-cleaned in O_3 for 180 s at 400 ℃ (▲), and initially pre-treated in NF_3 for 180 s at 400 ℃ (■), respectively.

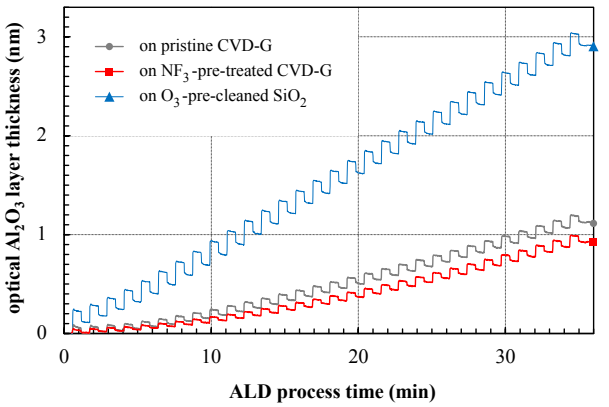

Figure 2. (color online) Optical Al_2O_3 layer thickness as determined by in-situ real-time Spectroscopic Ellipsometry (irtSE) in progression over the (TMA−H_2O, 400 ℃) ALD process time starting on a 100 nm SiO_2 substrate supporting a CVD graphene (CVD-G) monolayer that was initially pristine (•) and initially pre-treated in NF_3 for 180 s at 400 ℃ (■), respectively. The corresponding Al_2O_3 thickness course on an O_3-pre-cleaned (bare) SiO_2 starting substrate (▲) was re-drawn from Fig. 1 as a reference.

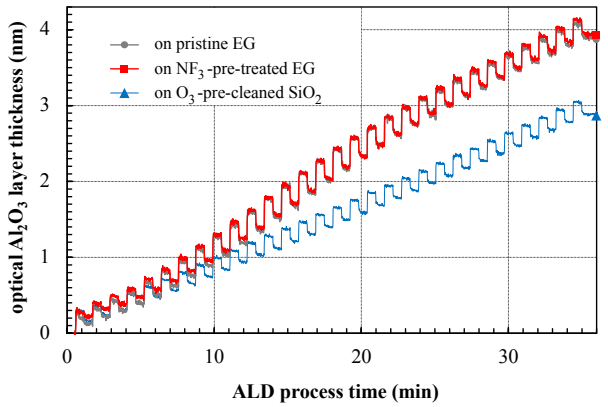

Figure 3. (color online) Optical Al_2O_3 layer thickness (N. B. the discussion in Sec. 4.3) as determined by in-situ real-time Spectroscopic Ellipsometry (irtSE) in progression over the (TMA−H_2O, 400 ℃) ALD process time starting on a Si-face n-type 4H-SiC substrate supporting an epitaxial graphene (EG) monolayer that was initially pristine (•) and initially pre-treated in NF_3 for 180 s at 400 ℃ (■), respectively. The corresponding Al_2O_3 thickness course on an O_3-pre-cleaned (bare) SiO_2 starting substrate (▲) was re-drawn from Fig. 1 as a reference.

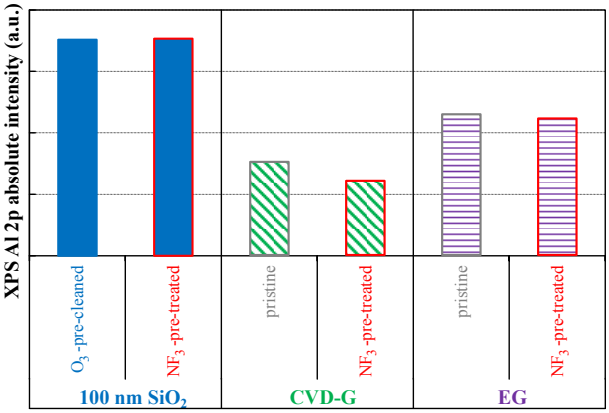

Figure 4. In-vacuo X-ray Photoelectron Spectroscopy (XPS) Aluminum (Al) 2p absolute peak intensity after 30 TMA−H_2O ALD cycles at 400 ℃ correspondingly starting on a 100 nm SiO_2 reference substrate, on a 100 nm SiO_2 substrate supporting a CVD graphene (CVD-G) monolayer, and on a Si-face n-type 4H-SiC substrate supporting an epitaxial graphene (EG) monolayer that accordingly was initially pristine, initially pre-cleaned in O_3 for 180 s at 400 ℃, or initially pre-treated in NF_3 for 180 s at 400 ℃.

In Fig. 3, the ALD started on a Si-face n-type 4H-SiC substrate supporting an epitaxial graphene (EG) monolayer. The GPC on EG displayed a rather unstable course over the 30 applied ALD cycles evolving to a seemingly higher value and accordingly larger final Al_2O_3 thickness (N. B. the discussion in Sec. 4.3) compared to the O_3-pre-cleaned (bare) SiO_2 reference. Absolutely no difference was observed by irtSE when the initial EG was pristine or pre-treated in NF_3 for 180 s at 400 ℃.

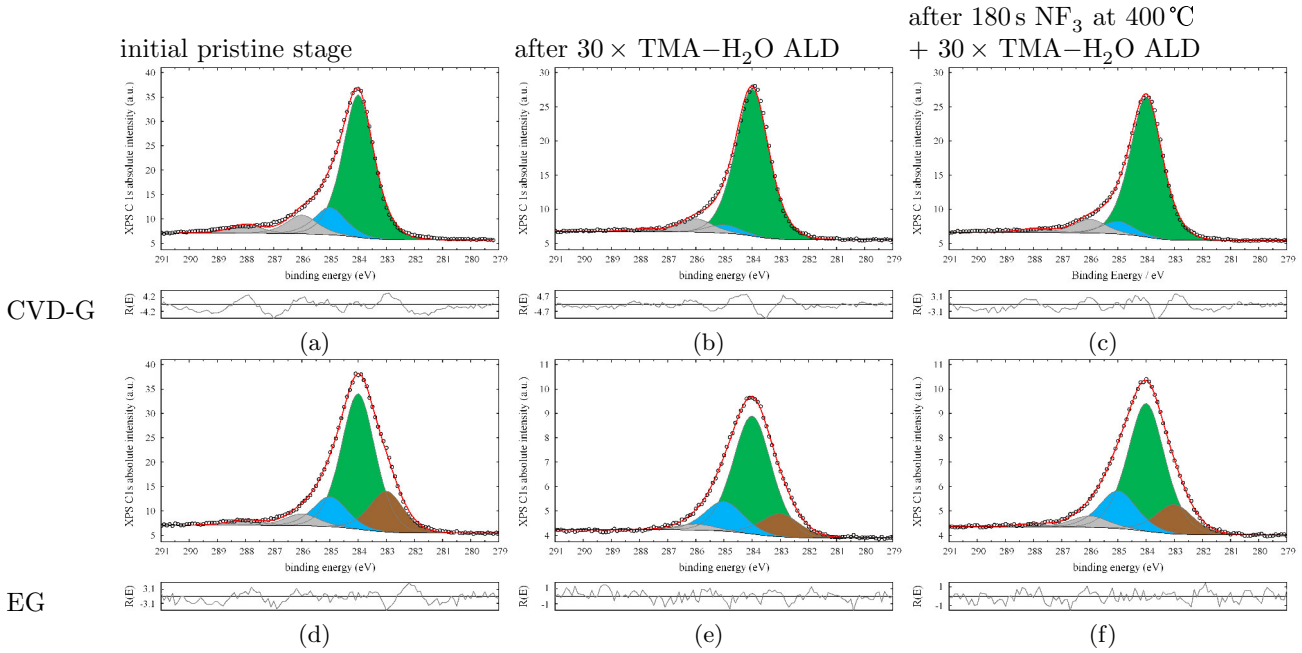

Figure 5. (color online) In-vacuo X-ray Photoelectron Spectroscopy (XPS) Carbon (C) 1s peak deconvolution for a 100 nm SiO_2 substrate supporting a CVD graphene (CVD-G) monolayer (a-c) and for a Si-face n-type 4H-SiC substrate supporting an epitaxial graphene (EG) monolayer (d-f) in their initial pristine stage (a, d), after 30 TMA−H_2O ALD cycles at 400 °C on the corresponding pristine surface (b, e), and after 30 TMA−H_2O ALD cycles at 400 °C succeeding 180 s NF_3-pre-treatment at 400 °C (c, f), respectively. The C−Si peak component at 283 eV is colored in brown, sp^2-hybridized C−C (i. e. the graphene monolayer) at 284 eV in green, sp^3-hybridized C−C or C−H at 285 eV in blue, C−O at 286 eV, and C=O at 288 eV in grey, respectively. The residuum between measurement (black circles) and peak fit (red solid line) is given below each spectrum.

3.2 In-vacuo X-ray Photoelectron Spectroscopy (XPS)

Fig. 4 gives the Aluminum (Al) 2p absolute peak intensity as revealed by in-vacuo XPS comparing the SiO_2 reference, CVD-G, and EG starting substrates as well as their different pre-treatments after 30 equally applied ALD cycles. On the SiO_2 reference, the most Al was found with no noticeable difference between an initial O_3-pre-clean or NF_3-pre-treatment. On CVD-G, the least Al was detected with even less Al when the ALD followed a NF_3-pre-treatment. On EG, more Al than on CVD-G but less than on the SiO_2 reference was measured with no noticeable difference between the ALD following no (on pristine EG) or following a NF_3-pre-treatment.

Fig. 5 depicts the in-vacuo XPS Carbon (C) 1s peak deconvolution comparing the CVD-G and EG monolayer in their initial pristine stage and after 30 equally applied ALD cycles following no and following a NF_3-pre-treatment, respectively. For a first estimate deconvolution, all C 1s peak components were assumed with fixed absolute binding energy positions (as given in the figure caption), same Full Width at Half Maximum (FWHM), no asymmetry but same Lorentzian-Gaussian mixing. For a more accurate evaluation and detailed discussion of XPS investigations on graphene, a link to Ref. 11, 18 needs to be given here. In the aggregate, CVD-G as well as EG showed a prominent C−C bond with sp^2-hybridization (green-colored component at 284 eV), which is typical for graphene and which did not disappear after any of the ALD coating procedures. Instead, the C 1s peak composition remained qualitatively unchanged for all the investigated samples. Just a decrease in the absolute C 1s peak intensity was observed after the ALD coating compared to the initial pristine stage.

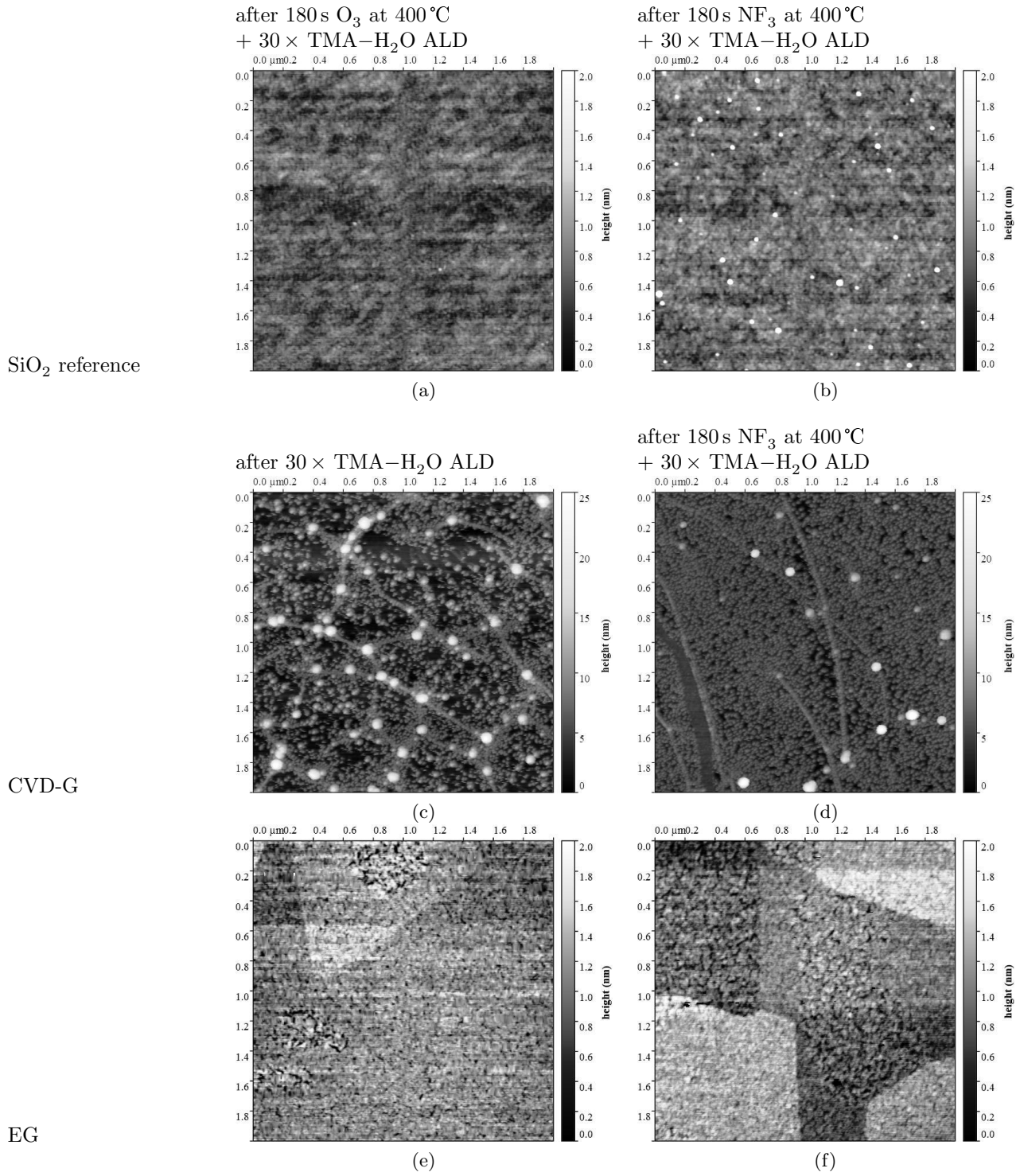

Figure 6. Surface topography as determined by Atomic Force Microscopy (AFM, 2 μm × 2 μm) on a 100 nm SiO_2 reference substrate (a, b), on a 100 nm SiO_2 substrate supporting a CVD graphene (CVD-G) monolayer (c, d), and on a Si-face n-type 4H-SiC substrate supporting an epitaxial graphene (EG) monolayer (e, f) after 30 TMA−H_2O ALD cycles at 400 ℃ succeeding 180 s O_3-pre-clean at 400 ℃ (a), after 30 TMA−H_2O ALD cycles at 400 ℃ on the corresponding pristine surface (c, e), and after 30 TMA−H_2O ALD cycles at 400 ℃ succeeding 180 s NF_3-pre-treatment at 400 ℃ (b, d, f), respectively. N. B. the distinct height scaling of 25 nm in (c) and (d) instead of 2 nm otherwise.

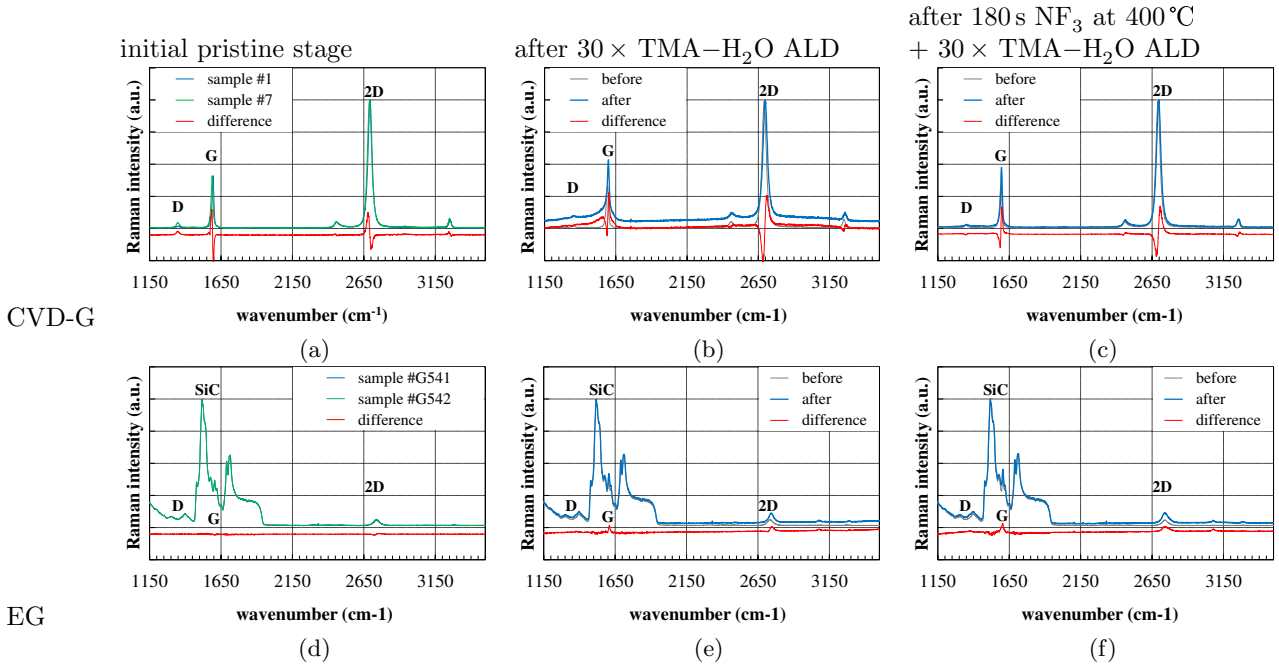

Figure 7. (color online) RAMAN spectra of a 100 nm SiO_2 substrate supporting a CVD graphene (CVD-G) monolayer (a-c) and of a Si-face n-type 4H-SiC substrate supporting an epitaxial graphene (EG) monolayer (d-f) in their initial pristine stage (a, d), after 30 TMA−H_2O ALD cycles at 400 °C on the corresponding pristine surface (b, e), and after 30 TMA−H_2O ALD cycles at 400 °C succeeding 180 s NF_3-pre-treatment at 400 °C (c, f), respectively. All intensities are normalized to the respective maximum intensity. The approximate positions of the D, G, and 2D bands are labeled accordingly. Each thin red line marks the difference between the measurements of various initial samples (a, d) and between after the corresponding coating procedure (thick blue line) minus before (grey line) (b, c, e, f), respectively.

3.3 Atomic Force Microscopy (AFM)

Fig. 6 assembles the Al_2O_3 morphology as determined by AFM after 30 equally applied ALD cycles following different pre-treatments on the SiO_2 reference, CVD-G, and EG starting substrates. On the SiO_2 reference, a continuous and very smooth (around 0.2 nm rms) film was found, nearly unaffected by the pre-treatment. On pristine CVD-G, a discontinuous and hence very rough (ca. 3.1 nm rms) coating was observed in the form of islands with low density and varying size preferentially localized at defect sites but occasionally also on the plane surface. On NF_3-pre-treated CVD-G, a discontinuous but moderately rough (ca. 1.8 nm rms) coating was achieved, which consisted of islands with rather high density and evenly distributed size preferentially on the plane surface and only occasionally at defect sites. On pristine and similarly also on NF_3-pre-treated EG, an almost continuous film with some pinholes and a low roughness (ca. 0.3 nm rms) was obtained.

3.4 Raman Spectroscopy

Fig. 7 arranges the RAMAN spectra of CVD-G and EG in their initial pristine stage and after 30 equally applied ALD cycles following no and following a NF_3-pre-treatment, respectively. For the pristine CVD-G, a negligible D band as well as a proper G-to-2D intensity ratio verified a nearly defect-free monolayer graphene. After either ALD coating procedure, the D band as well as the G-to-2D intensity ratio remained rather unchanged within the error of this measurement. However, a RAMAN mapping should clarify the representativeness of these spectra on CVD-G. For all the EG samples, strong signals from the SiC bulk superimposed the graphene-related D and G bands. Here, the spectrum of a bare SiC reference (without EG) should be measured and subtracted. Interestingly in the difference spectra between the measurements after the corresponding coating procedure on EG minus before (Fig. 7 e, f), a slight increase for the G band as well as an additional feature for the 2D band but no changes in the range of the D band were observed.

4. DISCUSSION

In Fig. 1-3, each increment of the optical Al_2O_3 layer thickness after completion of one entire (TMA−H_2O) ALD cycle could be interpreted as an amount of per-cycle-deposited Al_2O_3 material (also GPC). Similarly, the optical thickness increment per TMA exposure could be interpreted as an amount of TMA molecules that adsorbed at a respective surface. The thickness decrement per H_2O exposure could be assigned to a ligand removal from the TMA adsorbate thus creating the Al_2O_3 material. Notably in optical modeling of SE (Ψ, Δ) raw data, the optical Al_2O_3 layer thickness and an optical surface roughness were strongly correlated (i. e. a distinction between more material or a rougher morphology was impossible). As a consequence, the total amount of Al_2O_3 material that was deposited by the applied 30 ALD cycles and its morphology had to be individually verified by direct surface analysis as given in Fig. 4 by the in-vacuo XPS Al 2p absolute peak intensity and in Fig. 6 by the AFM surface topography, respectively.

4.1 Al_2O_3 ALD on 100 nm SiO_2 starting substrate references

In Fig. 1 on an O_3-pre-cleaned SiO_2 surface, a congruent GPC already from the very first ALD cycle indicated a nearly ideal linear growth initiation with no noticeable nucleation delay. The O_3-pre-clean removed all ambient C contaminations (from ca. 2 at.-% C in the pristine case towards below the detection limit) as evidenced by in-vacuo XPS (data not shown here). On an initially pristine and likewise on a NF_3-pre-treated SiO_2 surface, the very first TMA adsorption was reduced compared to the homogeneous linear Al_2O_3-on-Al_2O_3 growth regime resulting in a nucleation delay of approximately 5 ALD cycles. This substrate inhibition might be related to the contamination with ambient C. Consequently on SiO_2, neither a significant cleaning effect of NF_3 with respect to the removal of ambient C nor a provision of additional functional binding sites by NF_3 for a desired subsequently enhanced TMA adsorption could be deduced. AFM revealed a continuous (presumably pinhole-free) and very smooth Al_2O_3 ALD film formation on SiO_2 nearly unaffected by the studied pre-treatments.

4.2 Al_2O_3 ALD on transferred CVD graphene

In Fig. 2 on a CVD-G monolayer, a much reduced very first TMA adsorption compared to the O_3-pre-cleaned SiO_2 reference indicated CVD-G's lack of sufficient functional surface sites (i. e. dangling bonds) for the attachment of TMA. However, a tiny very first TMA adsorption was still observed, which might either be attributed to a TMA attachment at defects (like pinholes, grain boundaries, cracks, folded structures, etc.) leading to a specifically localized Al_2O_3 growth or attributed to a possible pyrolysis of TMA (at the substrate set-point temperature of 400 ℃) leading to a thermally induced random growth mode[19] and occurring rather unlocalized. In either case, the thus delayed nucleation seemed to continue beyond the 30 applied ALD cycles as the stable GPC of the homogeneous linear growth regime was not yet achieved. As cross-checked by in-vacuo XPS in Fig. 4, the least-detected total Al amount after 30 applied ALD cycles on CVD-G confirmed the least-achieved final Al_2O_3 thickness in Fig. 2 and hence also evidenced the strong CVD-G substrate inhibition.

In Fig. 6, AFM clarified the Al_2O_3 morphology on pristine CVD-G as islands, which has been directly related to the substrate-inhibited ALD growth mode according to Ref. 20. Nucleation sites, each of which a starting point for a later island formation, on pristine CVD-G were preferentially localized at defect sites and their density on the plane surface was comparably low. A NF_3-pre-treatment of CVD-G modified this appearance towards a higher density of nucleation sites preferentially on the plane surface. Apparently, the combination of a NF_3-pre-treatment with a possible TMA pyrolysis seemed to provide a positive effect for the ALD nucleation on CVD-G. However, compared to Ref. 6, our NF_3 dose (determined by exposure time and partial pressure) could still be increased in order to achieve an optimum Al_2O_3 coverage.

In-vacuo XPS in Fig. 5 in consistency with the RAMAN spectra in Fig. 7 verified the integrity of the CVD-G monolayer even after either coating procedure.

4.3 Al_2O_3 ALD on epitaxial graphene

In Fig. 3 on an EG monolayer, two issues in optical modeling the SE raw data occurred: First, the supporting SiC bulk substrate is transparent over a wide wavelength range (even in the visible) and was polished on both the front and back side, which induced FABRY-PÉROT oscillations in the SiC bulk due to backside reflections of the probing SE light; Second, each EG sample was mounted in a slightly lifted position (in order to suppress

additional FABRY-PÉROT oscillations in an air gap underneath the sample), so that the ALD coated both the front and back side, uncertainly probed by the backside-reflected SE light. In order to address these issues, cutting off the wavelength range, where SiC is transparent, as well as building an optical model for the FABRY-PÉROT interference in SiC failed up to now. In future experiments, a significant macroscopic roughening of the SiC backside would be needed or the backside should at least be covered with an opaque, vacuum-compatible, and temperature-stable material. As a first estimate in Fig. 3, our optical Al_2O_3 thickness on EG should be divided by two.

Nevertheless, a lowered GPC during the first 20 ALD cycles might gently suggest a substrate inhibition and thus might also indicate EG's lack of sufficient functional surface sites (i. e. dangling bonds) for the attachment of TMA. Equivalent to CVD-G, a comparably reduced very first TMA adsorption was observed. But other than CVD-G, EG has qualified as widely free of defects. Consequently, the very first TMA adsorption on EG might solely be attributed to the afore-mentioned pyrolysis of TMA leading to a thermally induced random growth mode.[19] The so-delayed nucleation seemed to be mostly completed after 20 ALD cycles as around that time the GPC stabilized to a value similar to the homogeneous linear growth regime. A cross-check by in-vacuo XPS in Fig. 4 revealed the total Al amount after 30 applied ALD cycles being around two third on EG compared to the SiO_2 reference and thus confirmed our estimation of a to-be-halved optical Al_2O_3 thickness on EG in Fig. 3.

In Fig. 6, AFM exhibited the morphology of Al_2O_3 on pristine and similarly on NF_3-pre-treated EG as an almost continuous film with some pinholes, which indicated an initially high density of nucleation sites on EG. This contradicted our expectations as well as all reports from present literature. Since we deposited at a much elevated substrate set-point temperature of 400 ℃, a possible TMA pyrolysis on EG seemed to randomly seed the following ALD. Speculatively, an intercalation of H_2O under the EG monolayer[21] could perhaps have promoted the ALD initiation further.

In-vacuo XPS in Fig. 5 in consistency with RAMAN spectroscopy in Fig. 7 suggested the integrity of the EG monolayer after either coating procedure. Though, the formation of a EG bilayer could not be excluded.

5. CONCLUSIONS

We tested the impact of NF_3 on CVD-G as well as EG monolayers prior to the ALD of Al_2O_3 at a substrate set-point temperature of 400 ℃. On both the graphene sources, irtSE in combination with AFM revealed a substrate inhibition with a resulting island formation. Hereby, the nucleation delay was shortest on EG but seemed to continue even beyond the 30 applied ALD cycles on CVD-G. This tendency was cross-checked by in-vacuo XPS and confirmed as the total-deposited Al amount was larger on EG compared to CVD-G. Furthermore, AFM revealed the Al_2O_3 morphology on CVD-G to be much improved by a NF_3-pre-treatment due to an increased density of nucleation sites, whereas on EG an almost continuous film indicated a high density of nucleation sites right from the start rather unaffected by a NF_3-pre-treatment. A thermally induced random growth mode component owing to a possible TMA pyrolysis on both the graphene surfaces was innovatively suggested. For all the investigated pristine as well as Al_2O_3-ALD-processed samples, the presence of a nearly defect-free CVD-G as well as EG monolayer was verified by in-vacuo XPS in consistency with RAMAN Spectroscopy.

ACKNOWLEDGMENTS

The authors kindly acknowledge the scientific assistance of Marion Geidel, Barbara Adolphi, Volker Neumann, Ingo Dirnstorfer, Mathias Schubert, Tino Hoffmann, Varun Sharma, and Ralf Tanner.

This work is supported by the German Research Foundation (DFG) 2013-2015 (GZ: BA 2009/3-1).

REFERENCES

[1] Vaziri, S., Lupina, G., Henkel, C., Smith, A. D., Östling, M., Dabrowski, J., Lippert, G., Mehr, W., and Lemme, M. C., "A Graphene-Based Hot Electron Transistor," *Nano Letters* **13**(4), 1435–1439 (2013).

[2] George, S. M., "Atomic Layer Deposition: An Overview," *Chemical Reviews* **110**(1), 111–131 (2010).

[3] Leskelä, M., Ritala, M., and Nilsen, O., "Novel materials by atomic layer deposition and molecular layer deposition," *MRS Bulletin* **36**(11), 877–884 (2011).

[4] Miikkulainen, V., Leskelä, M., Ritala, M., and Puurunen, R. L., "Crystallinity of inorganic films grown by atomic layer deposition: Overview and general trends," *Journal of Applied Physics* **113**(2), 021301 (2013).
[5] Puurunen, R. L., "Surface chemistry of atomic layer deposition: A case study for the trimethylaluminum/water process," *Journal of Applied Physics* **97**(12), 121301 (2005).
[6] Wheeler, V., Garces, N., Nyakiti, L., Myers-Ward, R., Jernigan, G., Culbertson, J., Eddy, C., and Kurt Gaskill, D., "Fluorine functionalization of epitaxial graphene for uniform deposition of thin high-k dielectrics," *Carbon* **50**(6), 2307–2314 (2012).
[7] Praxair Technology, Inc., "Xenon difluoride: Praxair Material Safety Data Sheet," (2009).
[8] Wenger, C., Kitzmann, J., Wolff, A., Fraschke, M., Walczyk, C., Lupina, G., Mehr, W., Junige, M., Albert, M., and Bartha, J. W., "Graphene based electron field emitter," *Journal of Vacuum Science & Technology B, Nanotechnology and Microelectronics: Materials, Processing, Measurement, and Phenomena* **33**(1), 01A109 (2015).
[9] Yakimova, R., Virojanadara, C., Gogova, D., Syväjärvi, M., Siche, D., Larsson, K., and Johansson, L. I., "Analysis of the Formation Conditions for Large Area Epitaxial Graphene on SiC Substrates," *Materials Science Forum* **645-648**, 565–568 (2010).
[10] Eriksson, J., Pearce, R., Iakimov, T., Virojanadara, C., Gogova, D., Andersson, M., Syväjärvi, M., Lloyd Spetz, A., and Yakimova, R., "The influence of substrate morphology on thickness uniformity and unintentional doping of epitaxial graphene on SiC," *Applied Physics Letters* **100**(24), 241607 (2012).
[11] Geidel, M., Junige, M., Adolphi, B., Wenger, C., Lupina, G., Yakimova, R., Darakchieva, V., Albert, M., and Bartha, J. W., "In-vacuo X-ray Photoelectron Spectroscopy for the investigation of pristine as well as pre-treated Graphene," in [*2015 E-MRS Spring Meeting and Exhibit*], (2015).
[12] Junige, M., Sharma, V., Schmidt, D., Albert, M., Schubert, M., and Bartha, J. W., "Progress in Spectroscopic Ellipsometry for the in-situ real-time investigation of Atomic Layer Depositions," in [*8th Workshop Ellipsometry*], (2014).
[13] Junige, M., Oddoy, T., Geidel, M., Darakchieva, V., Yakimova, R., Wenger, C., Lupina, G., Albert, M., Schubert, M., and Bartha, J. W., "In-situ real-time Spectroscopic Ellipsometry for the investigation of Atomic Layer Depositions on Graphene," in [*9th Workshop Ellipsometry*], (2015).
[14] Junige, M., Sharma, V., Schmidt, D., Pribil, G., Albert, M., Schubert, M., and Bartha, J. W., "In-situ real-time Spectroscopic Ellipsometry with 1.25 Hz sampling rate for the monitoring and control of kinetic processes in Atomic Layer Depositions," *Advanced Materials* (manuscript).
[15] Junige, M., Sharma, V., Tanner, R., Schmidt, D., Pribil, G., Albert, M., Schubert, M., and Bartha, J. W., "In-situ real-time monitoring and control of kinetic processes in Atomic Layer Depositions by Spectroscopic Ellipsometry with 1.25 Hz sampling rate," in [*2015 Frontiers of Characterization and Metrology for Nanoelectronics*], (2015).
[16] Junige, M., Geidel, M., Knaut, M., Albert, M., and Bartha, J. W., "Monitoring atomic layer deposition processes in situ and in real-time by spectroscopic ellipsometry," in [*IEEE 2011 Semiconductor Conference Dresden*], IEEE (2011).
[17] Knaut, M., Junige, M., Albert, M., and Bartha, J. W., "In-situ real-time ellipsometric investigations during the atomic layer deposition of ruthenium: A process development from [(ethylcyclopentadienyl)(pyrrolyl)ruthenium] and molecular oxygen," *Journal of Vacuum Science & Technology A: Vacuum, Surfaces, and Films* **30**(1), 01A151 (2012).
[18] Geidel, M., Junige, M., Adolphi, B., Wenger, C., Lupina, G., Yakimova, R., Darakchieva, V., Albert, M., and Bartha, J. W., "X-ray Photoelectron Spectroscopy for the investigation of Graphene in its pristine state and after several in-vacuo pre-treatments," *Advanced Materials* (manuscript).
[19] Puurunen, R. L., "Random Deposition as a Growth Mode in Atomic Layer Deposition," *Chemical Vapor Deposition* **10**(3), 159–170 (2004).
[20] Puurunen, R. L. and Vandervorst, W., "Island growth as a growth mode in atomic layer deposition: A phenomenological model," *Journal of Applied Physics* **96**(12), 7686 (2004).
[21] Ostler, M., Fromm, F., Koch, R. J., Wehrfritz, P., Speck, F., Vita, H., Böttcher, S., Horn, K., and Seyller, T., "Buffer layer free graphene on SiC(0001) via interface oxidation in water vapor," *Carbon* **70**, 258–265 (2014).